AGU PUBLICATIONS

JGR

Journal of Geophysical Research: Biogeosciences

RESEARCH ARTICLE
10.1002/2014JG002666

Key Points:
- Phenological indices explain variations in CO_2 exchange
- Start of the season dates explained variations in gross photosynthesis
- Peak CO_2 exchange rates best reflected variations in interannual CO_2 exchange

Correspondence to:
A. S. E. Kross,
angela.kross@mail.mcgill.ca

Citation:
Kross, A. S. E., N. T. Roulet, T. R. Moore, P. M. Lafleur, E. R. Humphreys, J. W. Seaquist, L. B. Flanagan, and M. Aurela (2014), Phenology and its role in carbon dioxide exchange processes in northern peatlands, *J. Geophys. Res. Biogeosci.*, *119*, 1370–1384, doi:10.1002/2014JG002666.

Received 15 MAR 2014
Accepted 26 JUN 2014
Accepted article online 1 JUL 2014
Published online 22 JUL 2014

Phenology and its role in carbon dioxide exchange processes in northern peatlands

Angela S. E. Kross[1], Nigel T. Roulet[2], Tim R. Moore[2], Peter M. Lafleur[3], Elyn R. Humphreys[4], Jonathan W. Seaquist[5], Lawrence B. Flanagan[6], and Mika Aurela[7]

[1]Science and Technology Branch-Earth Observation, Agriculture and Agri-Food Canada, Ottawa, Ontario, Canada, [2]Department of Geography, and Global Environmental and Climate Change Centre, McGill University, Montreal, Quebec, Canada, [3]Department of Geography, Trent University, Peterborough, Ontario, Canada, [4]Department of Geography and Environmental Studies, Carleton University, Ottawa, Ontario, Canada, [5]Department of Physical Geography and Ecosystem Science, Lund University, Lund, Sweden, [6]Department of Biological Sciences, University of Lethbridge, Lethbridge, Alberta, Canada, [7]Finnish Meteorological Institute, Helsinki, Finland

Abstract Ecosystem phenology plays an important role in carbon exchange processes and can be derived from continuous records of carbon dioxide (CO_2) exchange data. In this study we examined the potential use of phenological indices for characterizing cumulative annual CO_2 exchange in four contrasting northern peatland ecosystems. We used the approach of Jonsson and Eklundh (2004) to derive a set of phenological indices based on the daily time series of gross primary production (GPP), ecosystem respiration (R_e), and net ecosystem production (NEP) measured in the four peatland sites. The main objectives of this study were (a) to examine the variation in phenological indices across sites and (b) to determine the relationships among phenological indices, environmental conditions, and cumulative annual CO_2 exchange. The phenological index used to define the "start of the growing season" showed good potential for differentiation among sites based on their average annual site GPP. Sites with earlier growing seasons had the highest average annual site GPP. The "peak CO_2 exchange rate" phenological index performed best in reflecting variations among sites and for estimating annual values of GPP, R_e, and NEP (Pearson correlation coefficients ranged between 0.77 and 0.99, $p < 0.05$ for all.). The phenological indices and annual GPP, R_e, and NEP were sensitive to winter (January–March) and summer (July–September) temperature and precipitation, but correlations, though significant, were weak.

1. Introduction

Northern peatlands cover between 3 and 4% of the terrestrial landscape and contain between 250 and 700 Pg carbon (C) [e.g., *Tarnocai et al.*, 2002; *Yu et al.*, 2010]. They act as small persistent sinks for carbon dioxide (CO_2) and are sources of atmospheric methane [e.g., *Frolking et al.*, 2011]. Peatlands are potentially sensitive to climate change and variability [*Moore et al.*, 1998] because of the tight coupling between ecosystem structure, function, and their wetness [*Eppinga et al.*, 2009]. Since peatlands have C stores an order of magnitude greater than most other ecosystems, even relatively small changes in the net ecosystem production (NEP) could have global significance. There are few measurements of NEP for these ecosystems and few ecosystem models appropriate to simulate their C dynamics, in comparison with many other ecosystem types that store much less C. Most northern peatlands are relatively inaccessible so it is critical to improve models or to develop alternative C monitoring methods. Remote sensing approaches, for example, provide information about vegetation greenness and phenology which relate to patterns of CO_2 exchange.

Recent studies have shown the importance of phenology for ecosystem CO_2 exchange in forests [e.g., *Churkina et al.*, 2005; *Richardson et al.*, 2013; *Wu et al.*, 2012a, 2013] and wetlands [e.g., *Lund et al.*, 2009]. Longer growing seasons have been shown to be associated with increased gross primary production (GPP) and increased NEP [e.g., *Aurela et al.*, 2004; *Churkina et al.*, 2005; *Richardson et al.*, 2010]. Yet an increase in ecosystem respiration (R_e) can offset the increase in GPP, resulting in insignificant changes in NEP [e.g., *Moore et al.*, 2006], or alternatively, increases in R_e may exceed increases in GPP resulting in a net C loss to the atmosphere [e.g., *Piao et al.*, 2008; *Sacks et al.*, 2007].

Aurela et al. [2004] suggest that warming may increase the length of the growing season and consequently increase the C store of subarctic peatlands, but *Moore et al.* [2006] suggest that warmer springs will not have a strong impact on the annual C budget for temperate and boreal bogs, as earlier springs may not necessarily result in an increased use of solar radiation. *Lund et al.* [2009] examined patterns of NEP, GPP, and R_e derived

Table 1. Summary of the Different Phenological Indices Derived From the NEP, R_e, and GPP Time Series[a]

Classification	Phenological Indices	Phenological Interpretation	NEP[b]	R_e	GPP
Duration of phenological phases	Length of the growing season	Duration of photosynthetic activity			X
	C uptake period	Duration of net C uptake	X		
	Summer lag	Lag between the start of the growing season and the start of the C uptake period	X		X
	Autumn lag	Lag between the end of the growing season and the end of the C uptake period	X		X
Timing of phenological transitions	Start of the growing season	Start of measurable photosynthesis			X
	End of the growing season	End of measurable photosynthesis			X
	Start C uptake period	Start of net C uptake, switch from C source to C sink	X		
	End C uptake period	End of net C uptake, switch from C sink to C source	X		
	Date of annual peak CO_2 exchange rate (peak date)	Timing of the maximum measurable CO_2 exchange (center of the maturity phase)	X	X	X
CO_2 exchange rates at phenological transitions and phases	Annual peak CO_2 exchange rate (peak rate)	Maximum measurable level of CO_2 exchange (at the center of the maturity phase)	X	X	X
	CO_2 exchange recovery rate (recovery rate)	Level of CO_2 exchange during the recovery (i.e., green-up) period	X	X	X
	CO_2 exchange senescence rate (senescence rate)	Level of CO_2 exchange during the senescence period	X	X	X

[a]Phenological phases, transitions, and indices are synthesized from literature [*Reed et al.*, 1994; *Zhang et al.*, 2003; *Gu et al.*, 2003; *Jönsson and Eklundh*, 2004].
[b]These columns (NEP, R_e, and GPP) show which indices where extracted from which data sets.

from eddy covariance (EC) measurements across 12 peatland and tundra sites and developed seasonal correlations with environmental variables such as climate and vegetation characteristics and phenological indices. They reported significant correlations between the start and length of the growing season and the summer GPP and R_e across sites.

Previous phenology-C studies have mainly investigated the role of the length of the growing season or C uptake period and their transition dates (e.g., start and end of the growing season or C uptake period) on GPP and NEP. But continuous CO_2 exchange data allow the extraction of a set of phenological indices that are related to the rates of plant growth (reflected by rates of photosynthesis, respiration, and net ecosystem production) in addition to the timing and duration of plant growth phases. *Gu et al*. [2003] proposed an approach for analyzing ecosystem phenology using the changes in GPP time series. Using CO_2 exchange data from four forest sites and one grassland site, they estimated the daily maximum photosynthesis rate and developed phenological indices, such as the start, end and length of the growing season, and recovery and senescence rates of the CO_2 exchange (definition of these terms are in Table 1). *Jönsson and Eklundh* [2004] proposed a similar method for the analysis of ecosystem phenology derived from satellite sensor vegetation index (VI) time series; they also evaluated their method with EC flux data and soil moisture data. The advantage of these approaches is that they allow for the characterization of the seasonal CO_2 exchange dynamics through a variety of time-related (e.g., start of the season dates) and rate-related (e.g., peak photosynthesis rates) phenological indices. The variability of the indices across sites and years can provide information about the ecosystem plant community characteristics and its response to environmental conditions. Both studies focused mainly on the methodology of extraction of the phenological indices.

In this study, we examine the potential use of phenological indices for estimating cumulative annual CO_2 exchange at northern peatlands. We used the approach of *Jönsson and Eklundh* [2004] to derive a set of phenological indices from the times series of GPP, R_e, and NEP measured at four northern peatlands that are located in different climatic settings and that

have different vegetation characteristics. The main objectives of this study were (a) to examine the variation in phenological indices across sites and (b) to examine the relationships between phenological indices, temperature and precipitation, and cumulative CO_2 exchange. The intended goal of this analysis is to improve our understanding of the role of phenology in ecosystem CO_2 exchange processes in peatlands.

2. Sites

The peatland sites used in this study include an open bog (Mer Bleue, MB), a continental moderately rich treed fen (Labiche, LB), an open, moderately rich fen (Sandhill fen, SH), and a subarctic poor fen (Kaamanen, KM). MB, LB, and SH were part of the Canadian Carbon Program (http://www.fluxnet-canada.ca) while KM was part of the CarboEurope network (http://gaia.agraria.unitus.it/newtcdc2/GHG-Europe_home/Sites.aspx). Characteristics of these four sites are provided in Table 2. All sites were equipped with an EC flux tower providing continuous measurements of net ecosystem exchange of CO_2 (NEE), which were partitioned into R_e and GPP by the site investigators (MB: *Lafleur et al*. [2003] and *Roulet et al*. [2007], LB: *Flanagan and Syed* [2011], SH: *Sonnentag et al*. [2010], and KM: *Aurela et al*. [2004]). In this study we used gap-filled GPP, R_e, and NEP (~ −NEE), with a positive sign convention for all three measures. Positive values of NEP indicate uptake of CO_2 by the ecosystem. Both component fluxes of NEP were considered to be positive, for R_e positive values mean release of CO_2 to the atmosphere and for GPP positive values mean uptake of CO_2 from the atmosphere (i.e., NEP = GPP − R_e).

3. Methods

3.1. Phenological Indices

The methods of *Jönsson and Eklundh* [2004] and *Gu et al*. [2009] provide very similar phenological indices. Our decision to work with the method of *Jönsson and Eklundh* [2004] was mainly motivated by our previous experience with different phenology algorithms [*Kross*, 2005] and results from other studies [e.g. *Studer et al*., 2007; *White et al*., 2009] that show a more robust performance of the threshold-based methods than the local maximum or minimum (or maximum increase/decrease or maximum slope)-based methods for the estimation of ground phenological indices (using both satellite data and ground measurements). The approach used by *Gu et al*. [2009] is appealing because the local minimum and maximum reflect meaningful plant growth rates, but they are also sensitive to snow cover and may indicate snowmelt rather than green up in some cases [*Studer et al*., 2007], which is an issue with high-latitude peatlands.

We derived a set of phenological indices (Table 1 and Figure 1; see *Jönsson and Eklundh* [2004] for details) from daily GPP, R_e, and NEP using the TIMESAT software package [*Jönsson and Eklundh*, 2004], including start of the growing season, end of the growing season, length of the growing season, annual peak CO_2 exchange rates, date of the peak CO_2 exchange rates, green-up or recovery rates, and senescence rates (Figure 1) . Senescence rates are negative values, but for clearer comparisons and interpretation of results we used positive values throughout the text, figures, and analyses. The values of the start and end of the growing season were determined as the dates where daily GPP exceeded 5% of the seasonal amplitude (i.e., the difference between the curve minimum and maximum values). *Hird and McDermid* [2009] evaluated several smoothing methods for the estimation of the start of the growing season from simulated normalized difference vegetation index (NDVI) time series and reported the superior performance of the asymmetric Gaussian smoothing method of TIMESAT. This algorithm was used in our study. The 5% threshold has been used for the estimation of the start of the growing season based on climatological data and observations of the NEE in previous studies on wetlands [e.g., *Aurela et al*., 2004; *Lund et al*., 2009].

We also determined the C uptake period from the NEP time series (Table 1). The start of the C uptake period was defined as the day on which the daily smoothed NEP switched from negative to positive; the end of the C uptake period was defined as the day on which the smoothed NEP became negative again. The length of the C uptake period was calculated as the difference between the start and the end of the C uptake period. The spring lag was calculated as the difference between the start of the C uptake period and the start of the growing season; the autumn lag was calculated at the difference between the end of the growing season and the end of the C uptake period.

Journal of Geophysical Research: Biogeosciences 10.1002/2014JG002666

Table 2. Study Site Characteristics

Site Name	Lat. (°N)	Long. (°W)	Peatland Classification	TE/ ER/ KG Climate[a]	pH	Mean Annual Temperature: Long-Term[b] (Study Period) (°C)	Mean Annual Precipitation: Long-Term (Study Period) (mm)	Elevation Above Sea Level (m)	Years Used in the Analyses	LAI ($m^2\ m^{-2}$)	Dominant Vegetation[c]	Reference
Eastern peatland (Mer Bleue = MB)	45.41	75.52	Low-shrub ombrotrophic bog	MP/ H, HCT/ Dfb (26)	3.9–5.2	6.0 (6.7)	944 (942)	70	1998–2007	1.3	*Chamaedaphne calyculata*, *Ledum groenlandicum*, *Kalmia augustifolium* *Vaccinium myrtilloides*, *Sphagnum* spp.	*Moore et al.* [2002] and *Roulet et al.* [2007]
Western peatland (La Biche = LB)	54.95	112.47	Moderately rich treed fen	BP/ SH, LB/ Dfc (27)	6.2	2.1 (2.5)	504 (378)	577	2003–2009	2.6	*Picea mariana*, *Larix laricina*, *Betula pumila*, *Sphagnum* spp.	*Flanagan and Syed* [2011] and *Syed et al.* [2006]
Sandhill fen (SH)	53.80	104.62	Open moderately rich fen	BP/ SH, M-LB/ Dfc (27)	8.1	0.4 (1.8)	467 (518)	486	2003–2006	1.95	*Carex* spp, *Sphagnum* spp.	*Sonnentag et al.* [2010] and *Valentine* [1998]
Kaamanen (KM)	69.14	27.30	Subarctic poor fen	Dfc (27)	4.4	−1.3 (0.2)	395 (398)	155	2000–2005	0.7	*Betula nana*, *Ledum palustre*, *Empetrum nigrum*, *Sphagnum* spp.; *forbs*	*Aurela et al.* [2004]

[a]TE = Terrestrial ecozones Canada; ER = Ecoclimatic region Canada; KG = Koppen-Geiger. TE [*NRCan*, 2003]: BP, Boreal Plains; MP, Mixedwood Plains. ER [*Ecoregions Working Group*, 1989]: H, humid; HCT, high cool temperate; LB, low boreal; M–LB; middle-low boreal; SH, subhumid. KG [*Kottek et al.*, 2006]: D = snow; f = fully humid; b = warm summer; c = cool summer.
[b]Climate normals from the nearest Environment Canada weather station and from literature: Ottawa Macdonald-Cartier international airport, ON (MB), Athabasca, AB (LB), Waskesiu lake, SK (SH) and *Aurela et al.*, 2004 (KM).
[c]All sites have a ground cover of *Sphagnum mosses* and other mosses.
[d]Tree LAI 0.39 + Sedge/Shrub LAI 1.57.

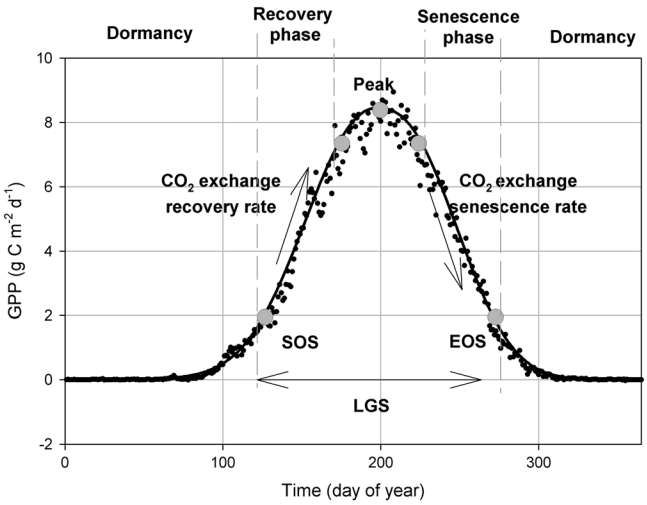

Figure 1. Example of TIMESAT phenological indices extracted from a GPP time series. Phenological indices shown in the illustration are the following: SOS = start of season; EOS = end of season; CO_2 exchange recovery rate (left slope); CO_2 exchange rate senescence (right slope); peak = peak CO_2 exchange rate; LGS = length growing season. Phenological phases: recovery phase = period of recovery (rapid increase) of CO_2 exchange, maturity phase = period of stability CO_2 exchange, and senescence phase = period of senescence (rapid decrease) of CO_2 exchange. Dots = EC measured GPP. Solid line = TIMESAT smoothed GPP. Phenological phases, transitions, and indices are synthesized from *Reed et al.* [1994], *Zhang et al.* [2003], *Gu et al.* [2003], and *Jönsson and Eklundh* [2004].

3.2. Analysis

To characterize the relationships between annual phenological indices, annual CO_2 exchange, and annual temperature and precipitation, we correlated all indices with annual cumulative GPP ($_{cum}$GPP), annual cumulative R_e ($_{cum}R_e$), and annual cumulative NEP ($_{cum}$NEP) and with monthly, seasonally, and annually averaged temperature and monthly, seasonally, and annually accumulated precipitation. We used the mean annual air temperature (MAT), annual total precipitation (TP), mean monthly temperatures (e.g., MT01 for mean temperature January) and total monthly precipitation (e.g., TP01 for January), seasonal temperature (means: e.g., MT0103 = January–March), and seasonal precipitation (totals: e.g., TP0406 = April–June). To represent seasons the year was divided into winter (January–March), spring (April–June), summer (July–September), and fall (October–December). Temperature and precipitation data were obtained from the nearest weather stations (Environment Canada stations for the Canadian sites; site station for KM). We used the Pearson correlation coefficient (r) to quantify the relationships between annual phenological indices, annual CO_2 exchange rates, and temperature and precipitation across site years. Because of the small number of site years, we used bootstrapped correlations to determine 95% confidence intervals for the correlation coefficients (confidence intervals that contained zero were not significant). To enable the evaluation of correlations across site years, we used annual anomalies of all variables calculated as the difference between the observed annual value and the observed value of the variable from a "pseudo-normal" year [e.g., *Richardson et al.*, 2010]. The pseudo-normal year was defined as the year with the smallest difference in temperature and precipitation from long-term normal temperature and precipitation at each site. For MB, LB, SH, and KM the pseudo-normal years were respectively 2004, 2009, 2003, and 2005.

We assessed the potential of phenological indices for monitoring CO_2 exchange using stepwise regressions to quantify the relationships between absolute values of annual phenological indices and absolute values of $_{cum}$GPP, $_{cum}R_e$, and $_{cum}$NEP across site years. For comparison of the phenological indices across peatlands we used summary statistics of the absolute values (i.e., not anomalies) of $_{cum}$GPP, $_{cum}R_e$, and $_{cum}$NEP for each site (site $_{cum}$GPP, site $_{cum}R_e$, and site $_{cum}$NEP, respectively) and summary statistics of absolute values of all phenological indices. We also used r (from bootstrapped correlations) to explore the relationships between phenology and CO_2 exchange among sites. All analyses were conducted using PASW Statistics 18, release version 18.0 (SPSS Inc. 2009, Chicago, IL).

4. Results and Discussion

4.1. Spatial Patterns in Phenology and CO_2 Exchange

There was a wide range in the start, end, and length of the growing season, as well as in the start, end, and duration of the C uptake period across the sites (Figures 2 and 3c). Within sites, the range of variation among years was smaller than the range of variation among sites with exception of the end of the C uptake period at SH and the end of the growing season at KM (Figures 2 and 3c). At MB and LB, the growing season and C uptake started about 1 month earlier than at SH and KM, and the C uptake period lasted 5–6 months. At SH

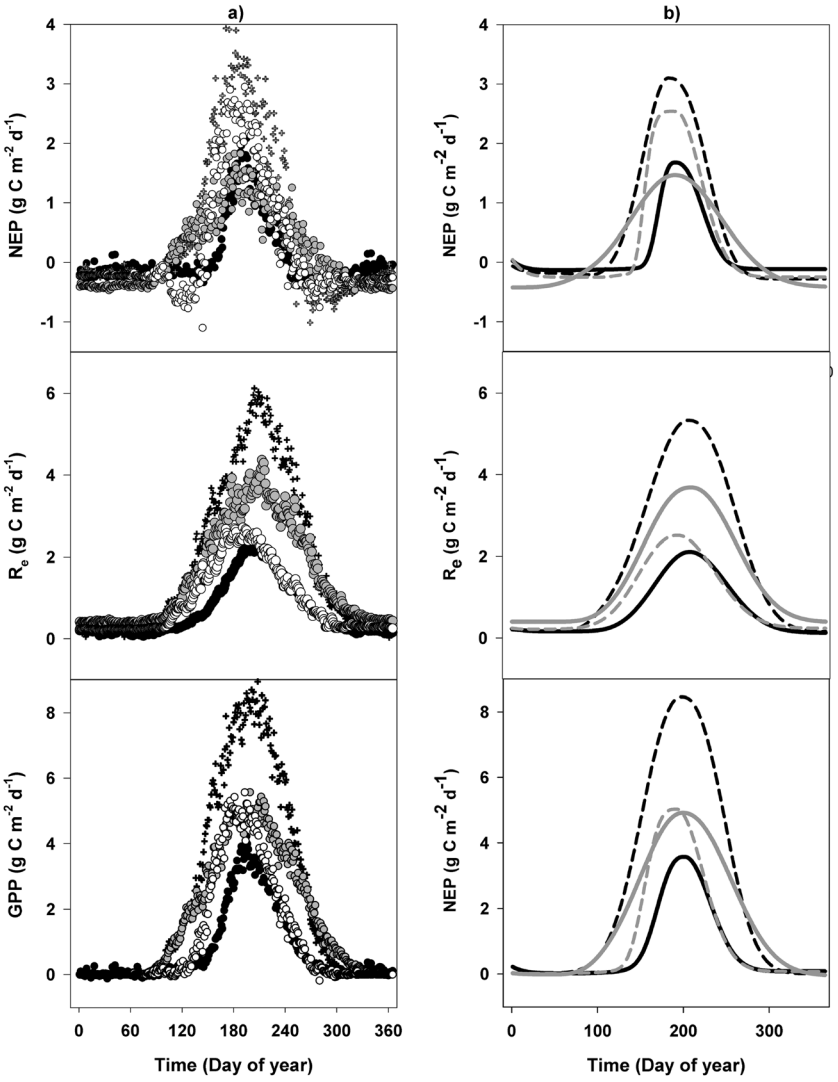

Figure 2. (a) Measured and (b) smoothed time series of NEP, R_e, and GPP. For Figure 2a, black dots = KM, black crosses = LB, grey dots = MB, and white dots = SH. Each dot represents the average CO_2 exchange for a specific day of year (across all available years per site). For Figure 2b, solid black line = KM, black dash line = LB, solid grey line = MB, and grey dash line = SH.

and KM, the C uptake period lasted 3–4 months (Figure 3c). C uptake started, on average, between 15 days (± standard deviation (SD); ±6 days) and 23 days (±12 days) after the start of the growing season and ended between 22 days (±15 days) and 63 days (±14 days) before the end of the growing season.

In spite of the wide range in the timing of the start and end of both the growing season and C uptake periods, all the sites reached their peak NEP (mean day of year (DOY) ± SD: DOY 192 ± 5 days), peak GPP (DOY 197 ± 4), and peak R_e (DOY 204 ± 7) around mid-July (Figure 3d), coinciding with the peak of the temperature (Figure 4) and 3 to 4 weeks after the annual peak of photosynthetically active radiation (data not shown). NEP was the first to peak, followed by GPP then R_e (Figure 3d). *Gu et al*. [2003] showed similar patterns for four forest sites and one grassland site, located in Finland, Canada, and USA (between 36 and 62°N). In their study, the peak GPP rate occurred between DOY 197 (grassland) and DOY 211, with a wide range in the start and end of the growing season and latitude.

Unlike previous findings [e.g., *Lund et al*., 2009], we found no significant correlations between the average start and length of the growing season and the average CO_2 exchange among the sites. The start of the growing season correlated best with average site $_{cum}$GPP ($r = -0.90$, $p < 0.1$, $n = 4$). A larger and wider distributed data set would be needed to verify these spatial relationships.

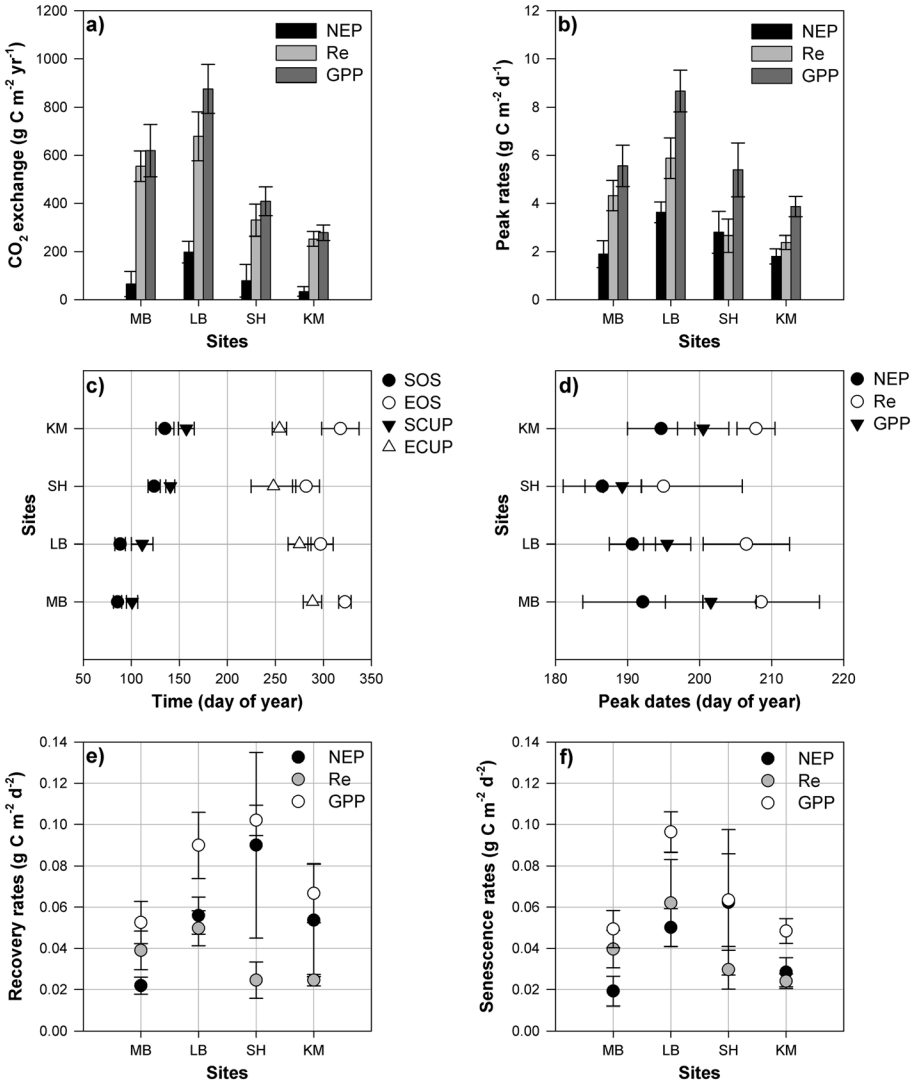

Figure 3. Summary statistics of the annual CO_2 exchange and phenological indices at the four peatlands. Sites sequences on the *X* axes and *Y* axes follow mean annual temperature with the highest being left (*x* axis) or bottom (*y* axis): (a) the annual total NEP, R_e, and GPP; (b) the annual peak NEP, R_e, and GPP; (c) the start of the growing season (SOS); the end of the growing season (EOS); the start of the C uptake period (SCUP) and the end of the C uptake period (ECUP); (d) the date of the peak NEP, R_e, and GPP; (e) the NEP, R_e, and GPP recovery rates (recovery rates are negative values but are shown as positive values in this figure), and (f) the NEP, R_e, and GPP senescence rates. The dots represent the annual average for each site, and the error bars represent 1 standard deviation.

Across the four sites, annual site CO_2 exchange varied considerably (mean annual flux ± mean standard deviation: GPP 278 ± 31 to 875 ± 101 g C m^{-2} yr^{-1}; R_e: 252 ± 30 to 679 ± 102 g C m^{-2} yr^{-1}; and NEP: 35 ± 19 to 198 ± 45 g C m^{-2} yr^{-1}) with LB having the largest and KM the smallest exchange for GPP, R_e, and NEP (Figure 3a). This pattern reflected the variations in average site leaf area index (LAI, Table 2) and is consistent with previous findings that showed the importance of vegetation characteristics, such as biomass and LAI for midsummer CO_2 exchange [*Humphreys et al.*, 2006], and geographic location, LAI, and pH for annual NEP [*Lund et al.*, 2009]. Comparing 12 peatland and tundra sites, *Lund et al.* [2009] reported highest GPP and largest annual CO_2 sink strength for two low-latitude sites with the highest LAI and pH. Leaf area determines the light absorption capacity at an ecosystem scale. Higher LAI allows for higher absorption and thus greater photosynthetic CO_2 uptake. While pH does not directly affect photosynthesis, it gives an indication of conditions (e.g., nutrient status) that can lead to high LAI and productivity [*Lund et al.*, 2009].

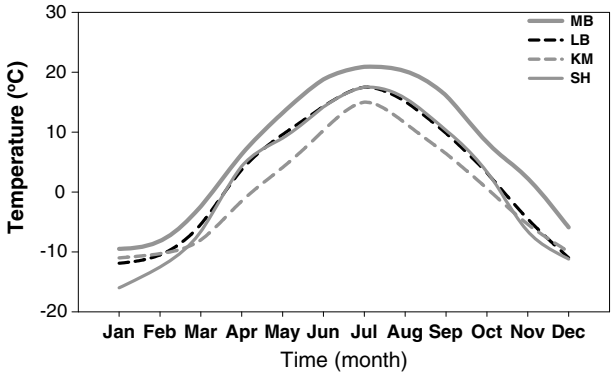

Figure 4. Average monthly temperatures of the four peatland sites. Monthly averages are calculated from all available years per individual site.

Peak rates showed a similar pattern as annual CO_2 exchange across the four sites (Figure 3b). There were strong correlations between peak NEP, R_e, and GPP and $_{cum}$NEP, $_{cum}R_e$, and $_{cum}$GPP across sites, respectively ($r = 0.93$, $p < 0.1$; $r = 0.99$, $p < 0.05$; and $r = 0.95$, $p < 0.05$, respectively, $n = 4$ for all). Peak GPP rates also correlated well with $_{cum}$NEP ($r = 0.98$, $p < 0.05$, $n = 4$). The importance of peak GPP rates for characterizing variations in annual GPP between different sites was also shown by *Gu et al.* [2009]. They studied the relationships between the peak canopy photosynthetic capacity (an index similar to our peak GPP) and the length of the growing season and the canopy C assimilation potential (index related to the annual cumulative GPP). Their results show the primary importance of the peak canopy photosynthetic capacity for the canopy C assimilation potential.

CO_2 exchange recovery and senescence rates showed variable patterns among sites. At MB and LB the growing season started at similar dates, but both the GPP recovery and senescence rates at LB were almost twice that of the corresponding rates at MB, and the vegetation at LB reached a higher peak GPP than the vegetation at MB (Figures 3e and 3f). At MB and LB, the average recovery rates were similar to the average senescence rates. SH and KM had similar start of growing season dates, but they were lagged compared with LB and MB. SH had the greatest GPP recovery rate of all sites and was the first to reach its peak GPP (Figures 3e and 3f). Both KM and SH displayed a certain amount of asymmetry in GPP and NEP with senescence rates about 60–70% of their corresponding recovery rates.

The highest GPP recovery and senescence rates were observed for SH and LB, followed by KM and MB (Figure 3e), reflecting the variation in LAI and pH values of the sites (Table 2). SH and LB have near-neutral pH values, while KM and MB are more acidic. *Gu et al.* [2009] suggest that GPP recovery rates reflect the efficiency of the vegetation to initiate photosynthesis in response to favorable environmental conditions. GPP senescence rates reflect the efficiency of the vegetation to maintain or transfer resources before leaf fall in response to nonfavorable environmental conditions. The variability of the average R_e recovery and senescence rates was small across all sites (Figures 3e and 3f), ranging between 0.03 and 0.04 g C m^{-2} d^{-2}. These findings suggest that the variability of the average NEP recovery and senescence rates depended more on the corresponding GPP rates than on the corresponding R_e rates. We also found a strong positive correlation between GPP senescence rates and $_{cum}$NEP ($r = 0.98$, $p < 0.05$, $n = 4$).

Future studies should evaluate the role of the GPP recovery rate in relation to LAI, pH, plant nitrogen, Rubisco, and chlorophyll content [e.g., *Yasumura et al.*, 2006] and the role of the GPP senescence rate in relation to leaf senescence mechanisms. Leaf senescence involves a series of events related to cellular disassembly in the leaf and the mobilization of materials released during this process, including nutrient resorption, which transfers nutrients from senescing leaves to storage organs or other tissues [*Aerts*, 1996]. In spring, remobilization of the directly available nutrients (from storage organs versus indirect nutrients from soil) can lead to competitive early regrowth of foliage [*Bausenwein et al.*, 2001a, 2001b]. All study sites included coverage of *Sphagnum* vegetation. LB and SH, the sites with the highest GPP recovery and senescence rates, had conifer trees (LB) and graminoids (SH) as dominant vegetation species. MB and KM were mainly dominated by evergreen shrubs, which have relatively lower nutrient resorption. Studies should further explore the role of nutrient resorption and dominant PFTs on GPP recovery and senescence rates.

4.2. Relationships Between Annual Phenology, CO_2 Exchange Rates, and Temperature and Precipitation

4.2.1. Relationships Between Phenology and CO_2 Exchange

C uptake is sensitive to both spring (e.g., bud burst, leaf unfolding, and start of the growing season [*Hänninen*, 1995; *Linderholm*, 2006; *Richardson et al.*, 2010; *Walther et al.*, 2002]) and autumn events (e.g., leaf senescence,

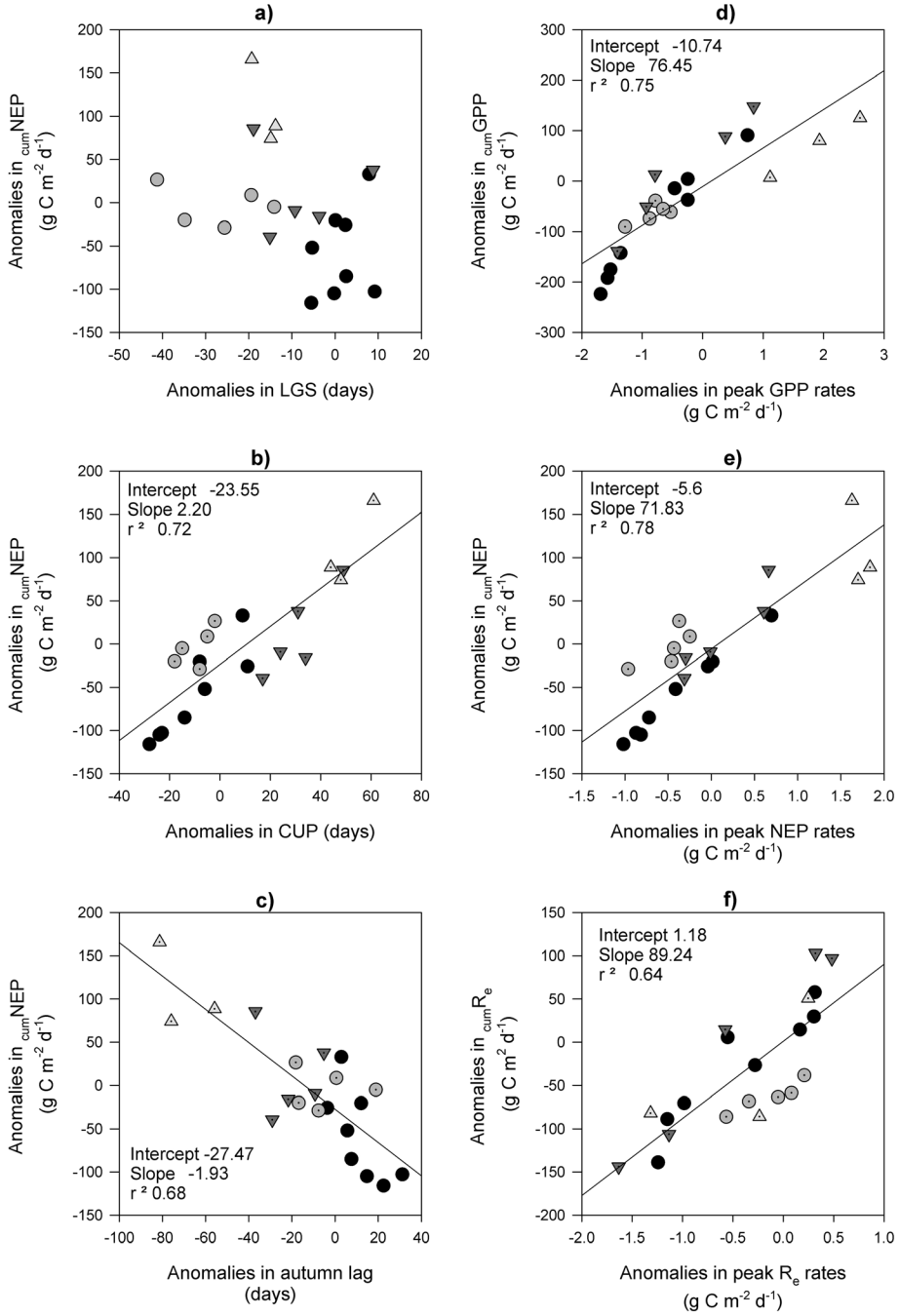

Figure 5. Scatterplots of anomalies in annual phenological indices and anomalies in $_{cum}$GPP, $_{cum}R_e$, and $_{cum}$NEP. Scatterplots, based on all 21 site years, are for the following: (a) anomalies in $_{cum}$GPP$_e$ or $_{cum}$NEP and LGS, (b) anomalies in $_{cum}$NEP and the C uptake period (CUP), (c) anomalies in $_{cum}$NEP and autumn lag, (d) anomalies in $_{cum}$GPP and peak GPP rates, (e) anomalies in $_{cum}$NEP and peak NEP rates, and (f) anomalies in $_{cum}R_e$ and peak R_e rates. Black dots = MB; grey dots = KM; dark grey inverted triangles = LB; light grey triangles = SH.

leaf fall, end of the growing season [*Piao et al.*, 2008; *Wu et al.*, 2013], and to the length of the growing season and C uptake period [e.g., *Aurela et al.*, 2004; *Churkina et al.*, 2005; *Richardson et al.*, 2009]). While the length of the growing season and its transitions reflect photosynthetic activity, the length of the C uptake period and its transitions reflect both respiration and photosynthetic activity. At our study sites, longer growing seasons were not associated with an earlier start of the season but with a later end of the season (data not shown). An earlier onset of the season and longer growing seasons were not associated with a longer C

Table 3. Pearson's Correlation Coefficients[a] for Relationships Between Anomalies in $_{cum}$GPP, $_{cum}R_e$, and $_{cum}$NEP and Anomalies in Phenological Indices[b]

Phenological Index	$_{cum}$GPP	$_{cum}R_e$	$_{cum}$NEP
Peak rate	.868[d]	.798[d]	.882[d]
Recovery rate	.472[c]	.670[d]	.578[d]
Senescence rate	.501[c]		−.547[c]
Start of C uptake period			−.604[d]
End of C uptake period			.756[d]
Length of C uptake period			.849[d]
Autumn Lag			−.826[d]
Peak date			.714[d]

[a]Correlation analyses relate anomalies across all site years, $n = 21$.
[b]Only significant correlations are shown.
[c]Significant at the 0.05 level.
[d]Significant at the 0.01 level.

uptake period nor an increased $_{cum}$GPP or $_{cum}$NEP. There were strong correlations between anomalies in the start and end of C uptake, and anomalies in the C uptake period, and between anomalies in the start, end, and length of the C uptake period and the autumn lag, and anomalies in $_{cum}$NEP (Figure 5 and Table 3). *Wu et al.* [2012a, 2012b, 2013] found similar significant correlations between the timing of the start and end of both the growing season and the C uptake period, the autumn lag, and annual NEP at deciduous and evergreen forest sites and suggested the autumn lag as the most promising predictor of annual NEP. The autumn lag, the time between the end of the C uptake period and the end of the growing season, reflects the balance between photosynthesis and respiration toward the end of the growing season. Shorter days, lower radiation, and cooler temperatures contribute to the decrease of photosynthesis rates during late summer [*Coursolle et al.*, 2006; *Frolking et al.*, 2009]. The autumn lag thus gives an indication of the time an ecosystem takes to initiate leaf fall as a response to decreasing photosynthesis and high respiration costs [*Wu et al.*, 2013]. Across site years, anomalies in $_{cum}$NEP correlated significantly with anomalies in GPP senescence rates ($r = 0.74$, $p < 0.01$, $n = 21$) and with anomalies in peak GPP rates ($r = 0.77$, $p < 0.01$, $n = 21$). Correlations were also strong and positive between anomalies in peak GPP rates and anomalies in $_{cum}$GPP, between anomalies in peak R_e rates and anomalies in $_{cum}R_e$, and between anomalies in peak NEP rates and anomalies in $_{cum}$NEP, across site years ($r = 0.87$, 0.80, and 0.88; $p < 0.01$ for all, $n = 21$) (Figure 5 and Table 3). Stepwise regressions showed the importance of the peak anomalies in combination with anomalies in: recovery rates for explaining variations in GPP ($r^2 = 0.85$, $p < 0.01$, $n = 21$), senescence rates for explaining variations in R_e ($r^2 = 0.72$, $p < 0.01$, $n = 21$), and the length of the growing season for explaining variations in NEP ($r^2 = 0.88$, $p < 0.01$, $n = 21$). Our findings are consistent with those of *Humphreys and Lafleur* [2011] who studied interannual variations in ecosystem-scale NEP at two low arctic tundra ecosystems. They found significant correlations between the maximum photosynthetic capacity and annual accumulated NEP at the two sites. Peak GPP is affected by leaf photosynthetic capacity and LAI, which are mainly controlled by nutrient and water availability [*Gu et al.*, 2009; *Noormets et al.*, 2009]. Variations in the annual length of the growing season are mainly determined by meteorological conditions (e.g., temperature and photoperiod). The greater importance of peak GPP (compared to the length of the growing season) for explaining variations in $_{cum}$NEP suggests that ecophysiological variables could be more important than temperature and photoperiod in controlling interannual variations in both $_{cum}$GPP and $_{cum}$NEP at our sites. Although the length of the growing season represents the potential for C assimilation, it is the ecophysiological variables that affect the photosynthetic activity that will determine the actual C assimilation over the growing season.

4.2.2. Effect of Temperature and Precipitation on Phenology and CO_2 Exchange

Variations in temperature, especially in the months before seasonal life cycle events, have been shown to be highly correlated with changes in plant phenology [e.g., *Penuelas and Filella*, 2001; *Tanja et al.*, 2003]. Studies have shown both significant [e.g., *Richardson et al.*, 2010] and nonsignificant [e.g., *Wu et al.*, 2012b] effects of spring temperatures on NEP and/or GPP in forest and nonforest (including cropland, grassland, and wetland) ecosystems. While spring warming is associated with increased annual NEP, autumn warming, on the contrary, would reduce annual NEP [e.g., *Piao et al.*, 2008].

Our results showed significant correlations between winter and summer temperatures and precipitation and phenological indices and CO_2 exchange. Higher temperatures in February and March were associated with an earlier start of the growing season (results not shown), and higher temperatures in March were associated with an earlier C uptake (Table 4). Warmer winters were associated with a longer C uptake period, shorter autumn lags, and higher peak NEP rates. Earlier and longer C uptake periods, shorter autumn lags, and higher peak rates were all associated with higher $_{cum}$NEP (Table 4) which may explain the significant correlations

Table 4. Significant Pearson's Correlation[a] Coefficients for Relationships Between Anomalies in Temperature and Precipitation and Anomalies in Phenological Indices

Phenological Index	Temperature	Precipitation
GPP peak rate	TP (.633[c]); TP0709 (.585[c])	MT08 (−.535[b])
R_e peak rate	MT07 (.50[b])	
NEP peak rate	MT08 (−.648[c]); MT02 (.624[c]); MT0103 (.588[c]); MT0709 (−.499[b])	TP (.700[c]); TP0709 (.675[c]); TP08 (.456[b])
GPP recovery rate	MT06 (.447[b]); MT (.436[b])	
R_e recovery rate	MT06 (.450[b])	TP01 (.457[b])
NEP recovery rate	MT08 (−.597[c])	TP0709 (.576[c]); TP (.483[b])
GPP senescence rate	MT08 (−.678[c]); MT02 (.610[c]); MT05 (−.436[b])	TP (.663[c]); TP0709 (.626[c])
NEP senescence rate	MT08 (.634[c]); MT02 (−.604[c]); MT0406 (.452[b]); MT05 (.434[b])	TP (−.570[c]); TP09 (−.545[b]); TP0709 (−.483[b])
NEP Start of the C uptake period	MT03 (−0.44[b])	TP0103 (0.44[b])
NEP End of the C uptake period	MT08 (−.634[c]); MT0103 (.631[c]); MT02 (.611[c]); MT0709 (−.594[c]); MT03 (.531[b]); MT05 (−.460[b])	TP09 (.584[c]); TP (.569[c]); TP0709 (.539[b]);TP02 (−.513[b])
NEP Duration of the C uptake period	MT08 (−.674[c]); MT0709 (−.646[c]); MT0103 (.635[c]); MT02 (.619[c]); MT03 (.600[c])	TP09 (.624[c]); TP0709 (.556[c]); TP02 (−.527[b]); TP (.484[b]); TP0103 (−.473[b])
NEP peak date	MT08 (−.861[c]); MT06 (−.719[c]); MT01 (−.568[c]); MT03 (.646[c]); MT0406 (−.597[c]); MT0709 (−.597[c])	TP08 (.683[c]); TP0709 (.618[c])
Autumn lag	MT08 (.816[c]); MT02 (−.669[c]); MT0709 (.610[c]); MT03 (−.608[c]); MT0103 (−.528[b]); MT05 (.446[b])	TP09 (−.778[c]); TP0709 (−.720[c]); TP (−.564[c]); TP08 (−.482[b])

[a]Correlation analyses relates anomalies across all site years, $n = 21$. Only correlations for the most important phenological indices (according to Table 4) are shown.
[b]Significant at the 0.05 level.
[c]Significant at the 0.01 level.
[d]MAT = mean annual air temperature; MT01 = mean temperature January; MT12 = mean temperature December; MT0103 = mean temperature from January to March; MT1012 = mean temperature from October to December; TP = total annual precipitation; TP01 = total precipitation January; TP12 = total precipitation December; TP0103 = total precipitation for January–March; TP1012 = total precipitation for October–December.

between winter temperatures and $_{cum}$NEP (Table 6). Warmer winters may translate into earlier snowmelt and/or could trigger earlier onset of vascular plant activity. High-nutrient resorption capacity may also cause peatland vegetation to start the photosynthesis mechanism in early spring. These findings are consistent with *Sottocornola and Kiely* [2010] who found that warmer winter soil temperatures in an Atlantic blanket bog led to an earlier onset of the season, which led to higher NEP and GPP, and warmer winters led to higher GPP.

Anomalies in $_{cum}$GPP correlated best with anomalies in the total precipitation in September ($r = 0.52$, $p < 0.05$); anomalies in $_{cum}R_e$ correlated best with anomalies in average June and July temperatures ($r = 0.52$ and 0.56, $p < 0.05$ and $p < 0.01$, respectively) (Table 5). Anomalies in $_{cum}$NEP were significantly correlated with anomalies in both precipitation and temperature: the average temperature in August and the total precipitation from July to September showed the highest correlations ($r = -0.80$ and 0.69, respectively, $p < 0.01$ for both) (Table 5 and Figure 6d). Peak GPP, R_e, and NEP rates showed similar sensitivity to the same weather variables (Table 4 and Figure 6b). Wetter summers were associated with a longer C uptake period (Table 4 and Figure 6a). Warmer and drier summers may lead to vegetation stress and decreased GPP, while R_e may increase under warmer conditions.

Table 5. Pearson's Correlation Coefficients[a] for Relationships Between Anomalies in Temperature and Precipitation, and Anomalies in $_{cum}$GPP, $_{cum}$*Re* and $_{cum}$NEP

	GPP	R_e	NEP
TP			.531*
MT02			.560[c]
MT03			.544[b]
MT06		.520[b]	
MT07		.564[c]	
MT08			−.795[c]
TP08			.546[b]
TP09	.524[b]		.630[c]
MT0709			−.657[c]
TP0709	.448[b]		.687[c]

[a]Correlation analyses relates anomalies across all site years, $n = 21$. Only significant correlations are shown. MT01 = mean temperature January …; MT12 = mean temperature December; MT0103 = mean temperature from January to March…; MT1012 = mean temperature from October to December; TP = total annual precipitation; TP01 = total precipitation January…; TP12 = total precipitation December; TP0103 = total precipitation for January–March; TP1012 = total precipitation for October–December.
[b]Significant at the 0.05 level.
[c]Significant at the 0.01 level.

A similar sensitivity to cooler and wetter summers led to shorter autumn lags (Table 4 and Figure 6c). *Wu et al.* [2012a] show the importance of the autumn lag for NEP in evergreen, broad leaf, and nonforest ecosystems (crops, grassland, and wetlands), but they did not find a significant relationship between

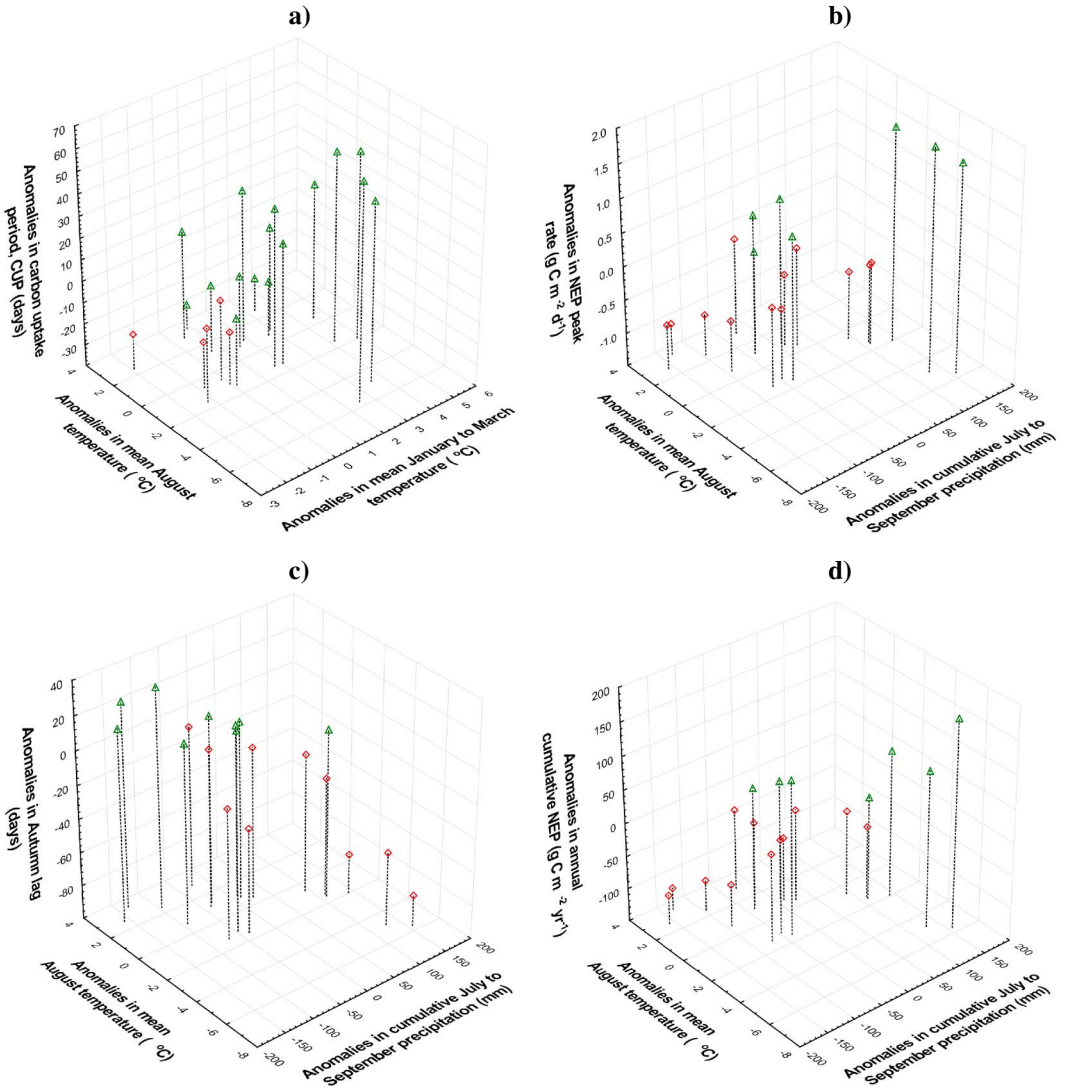

Figure 6. Variations in phenological indices, meteorological variables, and $_{cum}$NEP. (a) Variations in the C uptake period and temperature, (b) variations in peak NEP and temperature and precipitation, (c) variations in autumn lag and temperature and precipitation, and (d) variations in $_{cum}$NEP and temperature and precipitation. Diamonds are negative anomalies on the *z* axis; triangles are positive anomalies on the *z* axis.

spring (in their study: March to May) or autumn (in their study: September to November) warming and NEP. Yet NEP may be sensitive to other seasonal intervals than the ones used by *Wu et al.* [2012a]. Studies have used seasons (i.e., winter, spring, summer, and autumn) that are based on a variety of different time intervals, which can make it difficult to interpret the sensitivity of GPP, R_e, NEP, or phenological indices to meteorological variables. Future analyses should attempt to integrate temperature and precipitation over smaller windows (e.g., days, weeks, and months) or explore the definition of seasons based on temperature thresholds or vegetation phenology [e.g., *Lafleur et al.*, 1997].

4.3. Potential of Remote Sensing-Derived Phenology for C Monitoring in Peatlands

Our study illustrates the potential of several phenological indices for estimation of $_{cum}$NEP, $_{cum}$GPP, or $_{cum}R_e$ in northern peatlands. Most of these indices can be derived from satellite images, and several studies have shown the potential of remote sensing for deriving phenological indices, such as the length of the growing season and C uptake period and their transitions [e.g., *Churkina et al.*, 2005; *Garrity et al.*, 2011; *Richardson et al.*, 2009; *White et al.*, 2009], the autumn lag [*Wu et al.*, 2013], and peak, recovery, and senescence rates

Table 6. Coefficients of Determination (r^2) for Relationships Between $_{cum}$GPP, $_{cum}R_e$, and $_{cum}$NEP and Phenological Indices[a]

Phenological Indices	Predictors	r^2
$_{cum}$GPP	Peak GPP	.879[b]
	Peak GPP, LGS	.970[b]
	Peak GPP, LGS, SOS	.976[b]
$_{cum}R_e$	Peak R_e	.942[b]
$_{cum}$NEP	Peak NEP	.847[b]
	NEP Recovery rate	.909[b]

[a]Stepwise regression analysis relates absolute values of variables across all site years, $n = 25$.
[b]Significant at the 0.01 level.

[*Gu et al*., 2009; *Jönsson and Eklundh*, 2004]. Estimates of the timing of vegetation phenology at global scales are now available from the Moderate Resolution Imaging Spectroradiometer land cover dynamics product (MCD12Q2). Satellite-derived phenology was also used to infer variations in GPP and NEP [e.g., *Wu et al*., 2013; *Kross et al*., 2013].

Our study showed that variations in absolute peak rates related best to variations in absolute $_{cum}$NEP, $_{cum}$GPP, or $_{cum}R_e$ across all site years, accounting for at least 85% of the variations in $_{cum}$NEP, $_{cum}$GPP, or $_{cum}R_e$ (Table 6). Algorithms for deriving peak values are more straightforward than algorithms for deriving the timing of the start and end of the growing season and C uptake, or recovery and senescence rates. Previous studies have shown a wide variety in estimates of the start of the growing season depending on the phenology algorithm that was used [e.g., *White et al*., 2009]. Defining growing season transition points from continuous data is challenging, as most of the transitions are not clear and their extraction depends on a combination of smoothing algorithms, data-compositing methods, absolute and relative thresholds, inflection points, curvature, or local minima and maxima.

The peak is a visible feature of the continuous CO_2 exchange data. The annual maximum NDVI can be determined as the annual maximum NDVI value from cloud-free multiday NDVI composites [e.g., *Blok et al*., 2011; *Maxwell and Sylvester*, 2012]. Daily data are often noisy; peak values may be derived as the maximum value after smoothing the data [*Gu et al*., 2003; *Jönsson and Eklundh*, 2004] or by using the 90th to 95th percentile value of the raw data (considering 10%–15% of outliers). More research is needed to assess the sensitivity of peak rates for these different methods. Satellite data can complement ground data (e.g., EC flux data and camera data) in studying visual phenology (i.e., leaf out) and "functional" phenology (i.e., start of photosynthetic activity or C uptake and peak photosynthetic rates).

5. Conclusions

We studied the spatial patterns in phenological indices and CO_2 fluxes and the relationships between anomalies in annual phenological indices, meteorological variables, and cumulative annual CO_2 for four northern peatlands. Using multiyear CO_2 flux measurements, we showed the importance of several phenological indices derived from the CO_2 flux records for characterizing and/or explaining the variability in spatial and annual $_{cum}$GPP, $_{cum}R_e$, and $_{cum}$NEP. We also showed the importance of meteorological variables for both phenology and CO_2 uptake. Our main findings are the following:

1. An earlier start of the growing season and longer growing seasons were not associated with an increased C uptake period, or increased GPP or NEP among sites and interannually. But the start of the growing season can play an important role for the among-site differentiation of peatlands with regard to their average $_{cum}$GPP. Sites with the earliest start of the growing season had the highest average $_{cum}$GPP. Sites with a later start of the growing season (35–49 days later) had the lowest average $_{cum}$GPP.
2. GPP recovery and senescence rates may provide us with important information about spring ecosystem photosynthetic capacity and leaf fall mechanisms.
3. Both spatial and annual variations in $_{cum}$GPP, $_{cum}R_e$, and $_{cum}$NEP were best explained by variations in peak GPP, peak R_e, and peak NEP rates, respectively. NEP-derived phenological indices such as the C uptake period and its transitions and the autumn lag also showed some potential for explaining the variability of $_{cum}$NEP.
4. Peak rates, recovery rates, and senescence rates reflected variations in LAI and pH to some extent. Future studies should evaluate the role of these indices as indicators of LAI, pH, dominant PFTs, spring plant nitrogen content, Rubisco and chlorophyll content, and nutrient resorption.
5. Both phenology and CO_2 fluxes were more sensitive to winter (January–March) and summer (July–September) temperatures and precipitation than to spring and autumn temperatures and precipitation.
6. Understanding how phenological shifts will affect the C uptake in peatlands will improve our ability to predict future responses to changes in phenology most probably induced by climate change. All the

studied phenological indices can be derived from satellite reflectance data, and the future use of satellite-derived phenological indices for the study of CO_2 exchange in peatlands will allow us to assess relationships between peatland production and environmental conditions across inaccessible, large areas over long time periods. Future studies should explore methods for the derivation of peak values, and data sources should be evaluated with regard to their ability in reflecting variations in annual peak GPP, R_e, or NEP.

Acknowledgments

The flux data for this paper are available at the FLUXNET database (http://fluxnet.ornl.gov/): site names are AB = Western Peatland (LB), ON = Mer Bleue Eastern Peatland (MB), SK = Fen (SH), and FI = Kaa (KM). Meteorological data for the Canadian sites are available from Environment Canada (http://climate.weather.gc.ca/) and from the FLUXNET database for the Finnish site. We would like to thank A. Barr for providing the eddy covariance fluxnet data for the Sandhill fen and O. Sonnentag and A. Harris for reviewing the manuscript and providing valuable recommendations. This work was supported by fellowships for A. Kross from Natural Resources Canada-Canadian Centre for Remote Sensing and Fonds de Recherche du Québec-Nature et Technologies and the research grants to N.T. Roulet, T.R. Moore, J.W. Seaquist, P.M. Lafleur, E. Humphreys, and L.B. Flanagan from the Natural Sciences and Engineering Research Council of Canada and the Canadian Foundation for Climate and Atmospheric Sciences, and to M. Aurela from the European Commission, the Academy of Finland, and CARBOEUROFLUX and CARBOEUROPE-IP.

References

Aerts, R. (1996), Nutrient resorption from senescing leaves of perennials: Are there general patterns?, *J. Ecol.*, *84*(4), 597–608, doi:10.2307/2261481.

Aurela, M., T. Laurila, and J. P. Tuovinen (2004), The timing of snow melt controls the annual CO_2 balance in a subarctic fen, *Geophys. Res. Lett.*, *31*, L16119, doi:10.1029/2004GL020315.

Bausenwein, U., P. Millard, and J. A. Raven (2001a), Remobilized old-leaf nitrogen predominates for spring growth in two temperate grasses, *New Phytol.*, *152*(2), 283–290, doi:10.1046/j.0028-646X.2001.00262.x.

Bausenwein, U., P. Millard, B. Thornton, and J. A. Raven (2001b), Seasonal nitrogen storage and remobilization in the forb *Rumex acetosa*, *Funct. Ecol.*, *15*(3), 370–377, doi:10.1046/j.1365-2435.2001.00524.x.

Blok, D., G. Schaepman-Strub, H. Bartholomeus, M. M. P. D. Heijmans, T. C. Maximov, and F. Berendse (2011), The response of Arctic vegetation to the summer climate: Relation between shrub cover, NDVI, surface albedo and temperature, *Environ. Res. Lett.*, *6*(3), 035502, doi:10.1088/1748-9326/6/3/035502.

Churkina, G., D. Schimel, B. H. Braswell, and X. Xiao (2005), Spatial analysis of growing season length control over net ecosystem exchange, *Global Change Biol.*, *11*(10), 1777–1787, doi:10.1111/j.1365-2486.2005.001012.x.

Coursolle, C., et al. (2006), Late-summer carbon fluxes from Canadian forests and peatlands along an east–west continental transect, *Can. J. For. Res.*, *36*(3), 783–800, doi:10.1139/x05-270.

Ecoregions Working Group (1989), Ecoclimatic regions of Canada, first approximation. Ecological Land Classification Series, No. 23. Sustainable Development Branch, Conservation and Protection, Environment Canada, Ottawa, Ont. 199 pp. Report with map at 1:7.5 million scale.

Eppinga, M. B., P. C. de Ruiter, M. J. Wassen, and M. Rietkerk (2009), Nutrients and hydrology indicate the driving mechanisms of peatland surface patterning, *Am. Nat.*, *173*(6), 803–818, doi:10.1086/598487.

Flanagan, L. B., and K. H. Syed (2011), Stimulation of both photosynthesis and respiration in response to warmer and drier conditions in a boreal peatland ecosystem, *Global Change Biol.*, *17*(7), 2271–2287, doi:10.1111/j.1365-2486.2010.02378.x.

Frolking, S., N. T. Roulet, and D. Lawrence (2009), Issues related to incorporating northern peatlands into global climate models, in *Carbon Cycling in Northern Peatlands*, edited by A. J. Baird et al., 17 pp., AGU, Washington, D. C.

Frolking, S., J. Talbot, M. C. Jones, C. C. Treat, J. B. Kauffman, E.-S. Tuittila, and N. Roulet (2011), Peatlands in the Earth's 21st century climate system, *Environ. Rev.*, *19*, 371–396, doi:10.1139/a11-014.

Garrity, S. R., G. Bohrer, K. D. Maurer, K. L. Mueller, C. S. Vogel, and P. S. Curtis (2011), A comparison of multiple phenology data sources for estimating seasonal transitions in deciduous forest carbon exchange, *Agric. For. Meteorol.*, *151*(12), 1741–1752, doi:10.1016/j.agrformet.2011.07.008.

Gu, L., W. M. Post, D. D. Baldocchi, T. A. Black, S. B. Verma, T. Vesala, and S. C. Wofsy (2003), Phenology of vegetation photosynthesis, in *Phenology: An Integrative Science*, edited by M. D. Shwartz, pp. 467–485, Kluwer Academic Publishers, Dordrecht, Netherlands.

Gu, L., W. M. Post, D. D. Baldocchi, T. A. Black, A. E. Suyker, S. B. Verma, T. Vesala, and S. C. Wofsy (2009), Characterizing the seasonal dynamics of plant community photosynthesis across a range of vegetation types, in *Phenology of Ecosystem Processes*, edited by A. Noormets, Springer Science + Business Media, LLC, Springer, New York.

Hänninen, H. (1995), Effects of climatic change on trees from cool and temperature regions: An ecophysiological approach to modeling of bud burst phenology, *Can. J. Bot.*, *73*, 183–199, doi:10.1139/b95-022.

Hird, J., and G. J. McDermid (2009), Noise reduction of NDVI time series: An empirical comparison of selected techniques, *Remote Sens. Environ.*, *113*(1), 248–258, doi:10.1016/j.rse.2008.09.003.

Humphreys, E. R., and P. M. Lafleur (2011), Does earlier snowmelt lead to greater CO_2 sequestration in two low Arctic tundra ecosystems?, *Geophys. Res. Lett.*, *38*, L09703, doi:10.1029/2011gl047339.

Humphreys, E. R., P. M. Lafleur, L. B. Flanagan, N. Hedstrom, K. H. Syed, A. J. Glenn, and R. Granger (2006), Summer carbon dioxide and water vapor fluxes across a range of northern peatlands, *J. Geophys. Res.*, *111*, G04011, doi:10.1029/2005JG000111.

Jönsson, P., and L. Eklundh (2004), TIMESAT—A program for analyzing time-series of satellite sensor data, *Comput. Geosci.*, *30*(8), 833–845, doi:10.1016/j.cageo.2004.05.006.

Kottek, M., J. Grieser, C. Beck, B. Rudolf, and F. Rubel (2006), World map of the Köppen-Geiger climate classification updated, *Meteorol. Z.*, *15*(3), 259–263.

Kross, A. (2005), *Evaluating the Applicability of MODIS Data for Phenological Monitoring in the Netherlands*, 77 pp., Wageningen University and Research Centre, Wageningen.

Kross, A., J. W. Seaquist, N. T. Roulet, R. Fernandes, and O. Sonnentag (2013), Estimating carbon dioxide exchange rates at contrasting northern peatlands using MODIS satellite data, *Remote Sens. Environ.*, *137*, 234–243, doi:10.1016/j.rse.2013.06.014.

Lafleur, P. M., J. H. McCaughey, D. W. Joiner, P. A. Bartlett, and D. E. Jelinski (1997), Seasonal trends in energy, water, and carbon dioxide fluxes at a northern boreal wetland, *J. Geophys. Res.*, *102*(D24), 29,009–29,020, doi:10.1029/96JD03326.

Lafleur, P. M., N. T. Roulet, J. L. Bubier, S. Frolking, and T. R. Moore (2003), Interannual variability in the peatland-atmosphere carbon dioxide exchange at an ombrotrophic bog, *Global Biogeochem. Cycles*, *17*(2), 1036, doi:10.1029/2002GB001983.

Linderholm, H. W. (2006), Growing season changes in the last century, *Agric. For. Meteorol.*, *137*, 1–14, doi:10.1016/j.agrformet.2006.03.006.

Lund, M., et al. (2009), Variability in exchange of CO_2 across 12 northern peatland and tundra sites, *Global Change Biol.*, *16*(9), 2436–2448, doi:10.1111/j.1365-2486.2009.02104.x.

Maxwell, S. K., and K. M. Sylvester (2012), Identification of "ever-cropped" land (1984–2010) using Landsat annual maximum NDVI image composites: Southwestern Kansas case study, *Remote Sens. Environ.*, *121*, 186–195, doi:10.1016/j.rse.2012.01.022.

Moore, T. R., N. T. Roulet, and J. M. Waddington (1998), Uncertainty in predicting the effect of climatic change on the carbon cycling of Canadian peatlands, *Clim. Change*, *40*, 229–245, doi:10.1023/A:1005408719297.

Moore, T. R., J. L. Bubier, S. E. Frolking, P. M. Lafleur, and N. T. Roulet (2002), Plant biomass and production and CO_2 exchange in an ombrotrophic bog, *J. Ecol.*, *90*, 25–36, doi:10.1046/j.0022-0477.2001.00633.x.

Moore, T. R., P. M. Lafleur, D. M. I. Poon, B. W. Heumann, J. W. Seaquist, and N. T. Roulet (2006), Spring photosynthesis in a cool temperate bog, *Global Change Biol.*, *12*(12), 2323–2335, doi:10.1111/j.1365-2486.2006.01247.x.

Noormets, A., J. Chen, L. Gu, and A. Desai (2009), The phenology of gross ecosystem productivity and ecosystem respiration in temperate hardwood and conifer chronosequences, in *Phenology of Ecosystem Processes*, pp. 59–85, Springer, New York, doi:10.1007/978-1-4419-0026-5_3.

NRCan (2003), Atlas of Canada. Natural Resources Canada.

Penuelas, J., and I. Filella (2001), Phenology: Responses to a warming world, *Science*, *294*(5543), 793–795.

Piao, S., et al. (2008), Net carbon dioxide losses of northern ecosystems in response to autumn warming, *Nature*, *451*, 49–53, doi:10.1038/nature06444.

Reed, B. C., J. F. Brown, D. Vanderzee, T. R. Loveland, J. W. Merchant, and D. O. Ohlen (1994), Measuring phenological variability from satellite imagery, *J. Veg. Sci.*, *5*(5), 703–714, doi:10.2307/3235884.

Richardson, A. D., D. Y. Hollinger, D. B. Dail, J. T. Lee, J. W. Munger, and J. O'Keefe (2009), Influence of spring phenology on seasonal and annual carbon balance in two contrasting New England forests, *Tree Physiol.*, *29*, 321–331, doi:10.1093/treephys/tpn040.

Richardson, A. D., et al. (2010), Influence of spring and autumn phenological transitions on forest ecosystem productivity, *Philos. Trans. R. Soc., B*, *365*(1555), 3227–3246, doi:10.1098/rstb.2010.0102.

Richardson, A. D., T. F. Keenan, M. Migliavacca, Y. Ryu, O. Sonnentag, and M. Toomey (2013), Climate change, phenology, and phenological control of vegetation feedbacks to the climate system, *Agric. For. Meteorol.*, *169*, 156–173, doi:10.1016/j.agrformet.2012.09.012.

Roulet, N. T., P. M. Lafleur, P. J. H. Richard, T. R. Moore, E. R. Humphreys, and J. Bubier (2007), Contemporary carbon balance and late Holocene carbon accumulation in a northern peatland, *Global Change Biol.*, *13*(2), 397–411, doi:10.1111/j.1365-2486.2006.01292.x.

Sacks, W. J., D. S. Schimel, and R. K. Monson (2007), Coupling between carbon cycling and climate in a high-elevation, subalpine forest: A model-data fusion analysis, *Oceologia*, *151*, 54–68, doi:10.1007/s00442-006-0565-2.

Sonnentag, O., G. V. D. Kamp, A. G. Barr, and J. M. Chen (2010), On the relationship between water table depth and water vapor and carbon dioxide fluxes in a minerotrophic fen, *Global Change Biol.*, *16*(6), 1762–1776, doi:10.1111/j.1365-2486.2009.02032.x.

Sottocornola, M., and G. Kiely (2010), Hydro-meteorological controls on the CO_2 exchange variation in an Irish blanket bog, *Agric. For. Meteorol.*, *150*(2), 287–297, doi:10.1016/j.agrformet.2009.11.013.

Studer, S., R. Stockli, C. Appenzeller, and P. L. Vidale (2007), A comparative study of satellite and ground-based phenology, *Int. J. Biometeorol.*, *51*(5), 405–414, doi:10.1007/s00484-006-0080-5.

Syed, K. H., L. B. Flanagan, P. J. Carlson, A. J. Glenn, and K. E. Van Gaalen (2006), Environmental control of net ecosystem CO_2 exchange in a treed, moderately rich fen in northern Alberta, *Agric. For. Meteorol.*, *140*(1–4), 97–114, doi:10.1016/j.agrformet.2006.03.022.

Tanja, S., F. Berninger, and T. Vesala (2003), Air temperature triggers the recovery of evergreen forest photosynthesis in spring, *Global Change Biol.*, *9*, 1410–1426, doi:10.1046/j.1365-2486.2003.00597.x.

Tarnocai, C., I. M. Kettles, and B. Lacelle (2002), Peatlands of Canada Database. Geological Survey of Canada, Open File 4002.

Valentine, D. W. (1998), BOREAS TF-11 Biomass Data over the SSA-Fen, dataset. [Available at http://www.daac.ornl.gov] from Oak Ridge National Laboratory Distributed Active Archive Center, Oak Ridge, Tenn., doi:10.3334/ORNLDAAC/369.

Walther, G. R., E. Post, P. Convey, A. Menzel, C. Parmesan, T. J. C. Beebee, J. M. Fromentin, O. Hoegh–Guldberg, and F. Barlein (2002), Ecological responses to recent climate change, *Nature*, *416*(6879), 389–395, doi:10.1038/416389a.

White, M. A., et al. (2009), Intercomparison, interpretation, and assessment of spring phenology in North America estimated from remote sensing for 1982–2006, *Global Change Biol.*, doi:10.1111/j.1365-2486.2009.01910.x.

Wu, C., J. M. Chen, A. Gonsamo, D. T. Price, T. A. Black, and W. A. Kurz (2012a), Interannual variability of net carbon exchange is related to the lag between the end-dates of net carbon uptake and photosynthesis: Evidence from long records at two contrasting forest stands, *Agric. For. Meteorol.*, *164*, 29–38, doi:10.1016/j.agrformet.2012.05.002.

Wu, C., et al. (2012b), Interannual and spatial impacts of phenological transitions, growing season length, and spring and autumn temperatures on carbon sequestration: A North America flux data synthesis, *Global Planet. Change*, *92–93*, 179–190, doi:10.1016/j.gloplacha.2012.05.021.

Wu, C., et al. (2013), Interannual variability of net ecosystem productivity in forests is explained by carbon flux phenology in autumn, *Global Ecol. Biogeogr.*, *22*(8), 994–1006, doi:10.1111/geb.12044.

Yasumura, Y., K. Hikosaka, and T. Hirose (2006), Seasonal changes in photosynthesis, nitrogen content and nitrogen partitioning in *Lindera umbellata* leaves grown in high or low irradiance, *Tree Physiol.*, *26*(10), 1315–1323, doi:10.1093/treephys/26.10.1315.

Yu, Z., J. Loisel, D. P. Brosseau, D. W. Beilman, and S. J. Hunt (2010), Global peatland dynamics since the Last Glacial Maximum, *Geophys. Res. Lett.*, *37*, L13402, doi:10.1029/2010GL043584.

Zhang, X., M. A. Friedl, C. B. Schaaf, A. H. Strahler, J. C. F. Hodges, F. Gao, B. C. Reed, and A. Huete (2003), Monitoring vegetation phenology using MODIS, *Remote Sens. Environ.*, *84*(3), 471–475, doi:10.1016/S0034-4257(02)00135-9.